Acta Crystallographica Section D
Biological Crystallography
ISSN 0907-4449

Conformational stabilization and crystallization of the SecA translocation ATPase from *Bacillus subtilis*

Sevil Weinkauf,[a]* John F. Hunt,[b] Johannes Scheuring,[a] Lisa Henry,[c] John Fak,[b] Donald B. Oliver[d] and Johann Deisenhofer[c]

[a]Institut für Technische Chemie, Technische Universität München, Lichtenbergstrasse 4, D-85748 Garching, Germany, [b]Department of Biological Sciences, Columbia University, New York, NY 10027, USA, [c]Howard Hughes Medical Institute and Department of Biochemistry, University of Texas Southwestern Medical Center, Dallas, TX 75390-9050, USA, and [d]Department of Molecular Biology and Biochemistry, Wesleyan University, Middletown, CT 06459, USA

Correspondence e-mail: sevil.weinkauf@ch.tum.de

Received 25 September 2000
Accepted 16 January 2001

SecA is the peripheral membrane-associated subunit of the enzyme complex 'preprotein translocase' which assists the selective transport of presecretory proteins into and across bacterial membranes. The SecA protein acts as the molecular motor that drives the translocation of presecretory proteins through the membrane in a stepwise fashion concomitant with large conformational changes accompanying its own membrane insertion/retraction reaction cycle coupled to ATPase activity. The high flexibility of SecA causes a dynamic conformational heterogeneity which presents a barrier to growth of crystals of high diffraction quality. As shown by fluorescence spectroscopy, the T_m of the endothermic transition of cytosolic SecA from *Bacillus subtilis* is shifted to higher temperatures in the presence of 30% glycerol, indicating stabilization of the protein in its compact membrane-retracted conformational state. High glycerol concentrations are also necessary to obtain three-dimensional crystals suitable for X-ray diffraction analysis, suggesting that stabilization of the conformational dynamics of SecA may be required for effective crystallization. The SecA crystals grow as hexagonal bipyramids in the trigonal space group $P3_112$; they possess unit-cell parameters a = 130.8, b = 130.8, c = 150.4 Å at 100 K and diffract X-rays to approximately 2.70 Å using a high-flux synchrotron-radiation source.

1. Introduction

The selective transport of presecretory proteins across bacterial membranes is assisted by the membrane-bound multisubunit enzyme complex 'preprotein translocase' (den Blaauwen & Driessen, 1996). The *Escherichia coli* preprotein translocase consists of the peripheral translocation ATPase SecA (Cabelli *et al.*, 1988; Oliver, 1993) and the integral heterotrimeric membrane complex SecYEG (Hartl *et al.*, 1990; Joly *et al.*, 1994). SecYEG can associate with SecDFYajC (Duong & Wickner, 1997*a*,*b*), another integral heterotrimeric membrane protein which is not essential for protein translocation.

SecA is an essential protein that functions as the molecular motor driving the protein translocation process. Approximately half of the cellular SecA is located in the cytoplasm, while the remainder is either associated with the inner membrane or membrane-integrated (Cabelli *et al.*, 1991). SecA is functional as a homodimer (Driessen, 1993). Each monomer has a molecular weight of 102 kDa, comprising 901 amino acids, and contains a tandem pair of ATP-binding domain folds with sequence homology to the F1/RecA ATPase fold (Yoshida & Amano, 1995; Mitchell & Oliver, 1993). According to biochemical experiments, SecA can be

resolved into two major structural domains (den Blaauwen *et al.*, 1996; Price *et al.*, 1996): a 65 kDa N-terminal domain, which harbors the two ATP-binding domain folds and a segment that can be crosslinked to preproteins (Kimura *et al.*, 1991), and a 30 kDa C-terminal domain, which is involved in interactions with SecY (Snyders *et al.*, 1997), SecB (Fekkes *et al.*, 1997) and membrane (Breukink *et al.*, 1995).

According to the current model of translocation, the preprotein is delivered to the translocase in a cascade of targeting events including the association of the nascent chain to the export chaperone SecB and the binding of the SecB–preprotein complex to the translocase-associated SecA (Hartl *et al.*, 1990). The association of SecA with the membrane is mediated by its interaction with SecY and acidic phospholipids (Lill *et al.*, 1990; Breukink *et al.*, 1995). SecB–preprotein binding activates SecA for ATP binding, upon which a large conformational change occurs in SecA. This event is thought to drive the insertion of the C-terminal 30 kDa domain into the membrane (Economou & Wickner, 1994), which is observed to be tightly coupled to the translocation of an N-terminal loop of the bound preprotein, presumably through a channel formed by SecA and SecYEG (Joly & Wickner, 1993; Manting *et al.*, 2000). The release of the inserted preprotein from SecA is believed to occur upon hydrolysis of ATP; while the preprotein is not bound to SecA, proton-motive-force-driven transport of a further segment occurs (Driessen, 1992; van der Wolk *et al.*, 1997). Repeated cycles of ATP-driven and proton-motive-force-driven translocation stages result in the translocation of the entire preprotein through the membrane. SecDFYajC is thought to support preprotein translocation by regulating SecA membrane cycling (Duong & Wickner, 1997*b*).

The above model of the molecular mechanisms involved in protein translocation hypothesizes a very dynamic role for SecA: it is the molecular motor that pulls loops of presecretory protein through the membrane in a stepwise fashion concomitant with large conformational changes accompanying its own ATP-driven membrane insertion/retraction cycles. In this context, characterization of the atomic structure of SecA and of the nature of its intrinsic conformational changes are of exceptional interest. Despite the recent progress in characterization of the membrane component of the mammalian and yeast translocase, Sec61p (Hanein *et al.*, 1996; Beckmann *et al.*, 1997), SecYE of *B. subtilis* by electron microscopy (Meyer *et al.*, 1999) and the SecYEG complex of *E. coli* (Manting *et al.*, 2000), structural information on the SecA protein is still rare. Thin-sectioned crystals of *E. coli* SecA were analyzed by electron microscopy (Weaver *et al.*, 1992); however, the attained resolution of about 40 Å did not reveal structural details. Small-angle X-ray scattering was applied to study the shape and conformational flexibility of SecA in solution (Shilton *et al.*, 1998). In contradiction to earlier observations, this study postulated that the dimer has an elongated shape and that no detectable conformational changes occur upon interaction with nucleotides. Cytosolic SecA protein from *E. coli* has been refractory to crystallization attempts, possibly owing to excessive conformational flexibility or to heterogeneity caused by proteolysis of the N- and C-terminal regions of the protein (Weaver *et al.*, 1992).

The translocation machineries of *E. coli* and of *B. subtilis* share common features and consist of highly homologous proteins. The SecA proteins from both species are required for *in vivo* protein secretion and show striking similarities both functionally and structurally. The *B. subtilis* SecA, also called Div, is a homodimer of 96 kDa subunits comprising 841 amino acids (Takamatsu *et al.*, 1992). *E. coli* and *B. subtilis* SecA proteins show 71% identity over the first third of their sequences and 50% identity overall (Sadaie *et al.*, 1991). *B. subtilis* SecA is more hydrophilic and less susceptible to proteolysis, but its subcellular distribution is equivalent to that of *E. coli* SecA (McNicholas *et al.*, 1995). The N-terminal ATPase domain of *B. subtilis* SecA can substitute for the corresponding region from *E. coli* SecA. The stringent sequence conservation in the N-terminal domain combined with the strong overall homology imply that the two proteins have very similar tertiary structures. However, the more hydrophilic character, the smaller size and the reduced protease susceptibility of *B. subtilis* SecA indicated that this protein might be more amenable to crystallization.

In this context, we attempted to establish solution conditions favoring the formation of conformationally homogeneous populations of *B. subtilis* SecA suitable for crystallization. Here, we report the stabilization of the cytosolic SecA protein from *B. subtilis* by high concentrations of glycerol and the growth of high-quality three-dimensional crystals of the protein in this solution environment.

2. Purification of the SecA protein from *B. subtilis*

E. coli BL 21.19 cells harboring plasmid pT7(div) were grown in LB (pH 7.0) containing 0.1 mg ml^{-1} carbenicillin, 1 m*M* $MgSO_4$, 0.1 m*M* $CaCl_2$, 0.001% thiamine–HCl and 0.2% glucose at 303 K. An overnight culture in the same medium was diluted 1:100 into the large-scale culture and grown to an OD_{600} between 0.6 and 0.8 before induction of *B. subtilis* SecA expression for 2 h using 2 m*M* IPTG. The induced cultures were chilled on ice, harvested by centrifugation and rinsed in lysis buffer (100 m*M* NaCl, 1 m*M* EDTA, 1 m*M* DTT, 100 µg ml^{-1} PMSF, 1 µg ml^{-1} leupeptin, 1 µ*M* pepstatin, 50 m*M* Tris–HCl pH 7.6); the resulting cell pellet was flash-frozen in liquid nitrogen and and stored at 193 K pending protein purification.

All purification procedures were performed at 277 K. Frozen cells were thawed and resuspended in lysis buffer containing 20% glycerol and lysed by sonication. After ultracentrifugation at 45 000 rev min^{-1} for 1 h, the supernatant was filtered and applied to a DEAE Sepharose Fast Flow anion-exchange column (Pharmacia) equilibrated with buffer *A* (100 m*M* NaCl, 1 m*M* DTT, 0.025% NaN_3, 20% glycerol, 50 m*M* Tris–HCl pH 7.6). After an isocratic wash with buffer *A*, the column was eluted with a gradient of 0–100% buffer *B* (buffer *A* with 1 *M* NaCl). A single peak containing SecA was observed between approximately 5 and 20% buffer *B* depending on the preparation and all SecA-

Table 1
B. subtilis SecA data-collection statistics.

Standard definitions are used for all of the parameters (Drenth, 1994). Calculations were performed using the program *SCALEPACK* (Otwinowski & Minor, 1997). The mean value of $[I/\sigma(I)]$ was 2.1 in the limiting resolution shell between 2.75 and 2.69 Å, which is 100% complete for all measured reflections and 40% complete for reflections with $I = 2\sigma(I)$.

Space group	$P3_112$
Unit-cell parameters, 100 K (Å,°)	$a = 130.8$, $b = 130.8$, $c = 150.4$, $\alpha = 90$, $\beta = 90$, $\gamma = 120$
Data-collection statistics at 50.0–2.50 Å	
R_{sym} (%)	7.3 [$I = -3\sigma(I)$ for individual observations]
Mean redundancy	6.6
Completeness (%)	99.5 (all data)
Mean $I/\sigma(I)$	17.1

containing fractions, as analyzed by SDS–PAGE, were pooled. In order to avoid precipitation of SecA under low-salt conditions at high protein concentration, NaCl was added to the DEAE pool to a final concentration of 0.5 *M* prior to concentration in a Centriprep-50 ultrafiltration cell (Amicon) to a volume under 5 ml.

The concentrated sample was diluted tenfold in buffer *C* (25 m*M* NaCl, 1 m*M* DTT, 0.025% NaN_3, 20% glycerol, 50 m*M* HEPES pH 7.0) minus NaCl, filtered and applied to a Mono-S HR 10/10 cation-exchange column (Pharmacia) equilibrated in buffer *C*. After an isocratic wash with buffer *C*, the column was eluted with a gradient of 0–100% buffer *D* (buffer *C* with 1 *M* NaCl). SecA eluted as a broad and heterogeneous peak between approximately 10 and 30% buffer *D* depending on the preparation; the chromatogram always showed a series of sharp sub-peaks at partially reproducible positions within the envelope of the broad SecA peak and also a single sharp trough at a more variable position. This peak was divided and pooled in roughly two halves based on a shift in the pattern of weak lower molecular-weight bands observed in SDS–PAGE of the column fractions at a position which generally coincided with that of the sharp trough in the chromatogram. The weak lower molecular-weight bands are likely to derive from internal cleavages of the SecA polypeptide. The two pools from the broad SecA peak on the Mono-S column were handled separately in subsequent steps; crystals of higher quality were obtained from protein derived from the second half of the broad peak, which showed greater N-terminal homogeneity upon completion of the purification (see below).

Saturated $(NH_4)_2SO_4$ was added to each individual pool from the Mono-S column to a final concentration of 600 m*M*; the sample was then concentrated in a Centriprep-50 to a final volume of 2–5 ml, filtered and loaded onto a phenyl Superose HR 10/10 column (Pharmacia) equilibrated in buffer *E* [600 m*M* $(NH_4)_2SO_4$, 1 m*M* DTT, 0.025% NaN_3, 20% glycerol, 50 m*M* HEPES pH 7.5]. After an isocratic wash with buffer *E*, the column was eluted with a 120 ml linear gradient of 600–100 m*M* $(NH_4)_2SO_4$ in buffer *E*. SecA eluted as a single peak between 450 and 300 m*M* $(NH_4)_2SO_4$; this peak was characterized by a sharp rising edge but a trailing falling edge which also often showed a distinct shoulder. The protein was pooled without the trailing edge of the peak toward low $(NH_4)_2SO_4$ concentration, because N-terminal sequence analysis indicated very high amino-terminal heterogeneity (∼50%) in this region of the chromatogram.

The purified protein was exchanged into 300 m*M* $(NH_4)_2SO_4$, 1 m*M* DTT, 20 m*M* BES pH 7.0 by repeated cycles of concentration/dilution in a Centricon-50 ultrafiltration cell prior to concentration to 15–20 mg ml^{-1} for crystallization. The protein concentration in the crystallization stock was quantified based on absorbance at 280 nm (after dilution in the same buffer) using an extinction coefficient of 0.852 OD mg^{-1} ml^{-1}. The endogenous ATPase activity of SecA was tested as described by Lill *et al.* (1990).

3. Amino-terminal protein homogeneity controls the quality of SecA crystals

Once crystals of SecA were obtained under the conditions described below, extreme preparation-to-preparation variability was observed in their growth properties and limiting diffraction quality. Early in the project, the best crystals were obtained from a protein preparation showing approximately 20% content of SecA with a characteristic 50-residue C-terminal deletion as assessed by SDS–PAGE. Subsequent preparations showing no apparent covalent heterogeneity on gels yielded substantially poorer crystals which grew more slowly to a smaller limiting size and were characterized by weaker intrinsic diffraction power based on the scaling *B* factor for their diffraction data relative to a reference crystal. To emulate the situation observed in a partially C-terminally truncated protein preparation, crystals were grown from a mixture of approximately 80% full-length wild-type protein plus 20% protein engineered to have a 46-residue C-terminal truncation. The best diffraction data for SecA (Table 1) were ultimately obtained from this mixture. However, crystals of only very slightly diminished quality (∼0.1 Å in limiting resolution) were consistently obtained from pure full-length wild-type protein, so that the role of the C-terminal truncation in enhancing the lattice quality remains ambiguous. Nonetheless, these data, combined with the data on the importance of the N-terminus (see below), suggest that the enhancement in crystal quality observed during long growth periods is unlikely to result from slow proteolysis during storage at 299 K. The gradual improvement in SecA crystal quality could result from a wide variety of other factors such as slow chemical modification (deamidation or oxidation) or lattice annealing, perhaps owing to a slow local conformational change or the gradual increase in ammonium sulfate concentration as the well slowly dehydrates.

These surprising observations led us to undertake a retrospective analysis of the N-terminal protein sequence in several preparations yielding crystals of widely varying quality. The analysis indicated an unambiguous correlation between the N-terminal homogeneity of the protein and the ultimate quality of the crystals derived from that preparation. Preparations showing more than 15% total of fragments

starting at residue 5 and residue 7 of SecA did not yield crystals suitable for use. In contrast, and as mentioned above, even a major truncation of 50 amino acids at the carboxy-terminus had no apparent influence on the crystal quality. This behaviour could be rationalized once the crystal structure was obtained based on participation of the N-terminal amino acids in a dimer contact and the complete disorder of the final 40 residues in the protein (manuscript in preparation).

However, identification of the controlling role of the amino-terminus of SecA in modulating crystal quality played a critical role in the structure-determination project by allowing a robust purification method to be developed which yielded protein with very reproducible crystallization properties. SecA protein from *B. subtilis* shows considerable heterogeneity during column chromatography and we sought to establish the relationship between this heterogeneity and the N-terminal homogeneity as a rational approach to the development of an improved purification protocol. On all the columns used (ion exchange and hydrophobic interaction), SecA shows considerable variation in its elution position depending on the protein concentration in the load, indicating dynamic heterogeneity in its aggregation state during chromatography. Its elution profiles are anomalously broad on both cation-exchange and hydrophobic interaction columns. N-terminal sequencing of protein derived from the leading *versus* trailing edges of these broad peaks indicated systematic differences in the level of N-terminal homogeneity in different parts, with the first half of the cation-exchange peak showing somewhat reduced homogeneity compared with the second half and the trailing edge of the hydrophobic interaction peak showing drastically increased heterogeneity (more than 50%) compared with the leading edge.

Based on this analysis, the cation-exchange peak was pooled in two halves which were then purified separately by hydrophobic interaction chromatography, where the trailing edge of the peak was discarded. Fully purified protein from the first half of the cation-exhange peak generally yielded protein that was 85% intact at the N-terminus, while the fully purified protein from the second half of the cation-exhange peak generally yielded protein that was close to 95% intact at the N-terminus.

4. Effect of glycerol on *B. subtilis* SecA stability

An endothermic conformational transition occurs slightly above physiological temperature in soluble SecA from both *E. coli* and *B. subtilis* as shown by differential scanning calorimetry and fluorescence measurements (Ulbrandt *et al.*, 1992). This transition is likely to be a conserved feature of the conformational reaction cycle of SecA, as it presumably represents the conversion of the enzyme into its membrane-associating conformation (Ulbrandt *et al.*, 1992; den Blaauwen *et al.*, 1996; Ramamurthy *et al.*, 1998). This conversion involves a partial unfolding event and is likely to correspond to an extreme conformational excursion of the enzyme relative to the compact conformation that is predominant at room temperature and that is immobilized in the protein lattice upon crystallization. Indeed, fluorescence anisotropy measurements combined with site-directed tryptophan mutagenesis have shown that one subdomain of *E. coli* SecA dissociates from the core of the enzyme and enters a higher mobility state during the endothermic transition (manuscript in preparation), consistent with the earlier observation of strongly enhanced susceptibility to proteolysis in this conformational state (Ulbrandt *et al.*, 1992; Song & Kim, 1997). In order to investigate whether glycerol stabilizes the compact protease-resistant conformation of SecA, fluorescence spectroscopy was used to monitor the effect of this cosmotropic additive on the progress of the endothermic conformational transition of SecA.

For fluorescence spectroscopy, 1.5 ml samples contained 0.5 µ*M* SecA monomer in 50 m*M* KCl, 1 m*M* $MgCl_2$, 25 m*M* Tris–HCl pH 8.0 and variable glycerol concentration as indicated. The protein concentration was determined by absorbance spectroscopy following dilution of a small volume of the parental protein stock into 6 *M* guanidinium–HCl, 20 m*M* Na_2HPO_4 pH 6.5, using an *a priori* extinction coefficient of 0.526 OD mg^{-1} ml^{-1}. Total fluorescence emission spectra were collected on a QuantaMaster C-61 spectrofluorimeter from PTI with T-format optics using 280 nm excitation and 4 nm slits with a 1 nm step size and a 0.5 s integration time. At each glycerol concentration and temperature a polarized emission spectrum was collected from 300 to 400 nm; total fluorescence was calculated as the sum of the parallel emission plus two times the perpendicular emission (after buffer subtraction and suitable correction for the different sensitivity of the two emission channels). The resulting total fluorescence spectrum was smoothed in a 21-point window prior to extracting the emission intensity at 340 nm. Spectra were collected from 297 to 325 K in 2 K steps with 5 min intervals. The T_m values were calculated by fitting two linear least-squares baselines to suitable regions of the titration curves on either side of the endothermic transition. These baselines were used to infer the relative occupancy of the two conformational states by assuming a simple two-state model of the transition based on the position of the observed fluorescence intensity relative to the high-temperature and low-temperature baselines; the logarithm of the equilibrium constant inferred in this way was plotted *versus* temperature in the transition region and a linear least-squares fit was used to calculate the T_m, *i.e.* the temperature at which the logarithm of the equilibrium constant is zero.

Fluorescence titrations were performed on *B. subtilis* SecA protein in the presence of 0–30%(*v*/*v*) glycerol (Fig. 1*a*). The thermal titration curves show a transition in the range 308–323 K, with a progressive shift to higher temperatures with increasing glycerol content. The T_m values determined from these titrations are plotted as a function of the glycerol concentration in Fig. 1(*b*). In the absence of glycerol, the T_m value for the endothermic transition of *B. subtilis* SecA was observed to be 314.9 K, which is similar to that of its *E. coli* counterpart. A modest glycerol concentration of 10%(*v*/*v*) resulted in a slight increase of the T_m to 316.1 K, but a much more significant increase was observed at glycerol concen-

trations of 25% and 30%(*v*/*v*), which moved the T_m to 319.3 and 319.6 K, respectively. While the data in Fig. 1 were collected using an excitation wavelength of 280 nm to yield combined tryptophan/tyrosine fluorescence emission spectra, equivalent results were observed in the weaker emission spectra recorded using selective 297 nm excitation of the two tryptophans in *B. subtilis* SecA (not shown).

These data showing a 4.7 K increase in the T_m of the endothermic transition of the enzyme indicate substantial stabilization of the compact protease-resistant conformation of *B. subtilis* SecA by high concentrations of glycerol. In this context, it is noteworthy that the trigonal crystal form of the enzyme could only be grown in the presence of glycerol at a concentration of 25% or higher (see below).

5. Crystallization and preliminary X-ray analysis of SecA

A variety of precipitants and additives as well as large pH and temperature ranges were tested in seeking crystallization conditions for *B. subtilis* SecA. In the absence of glycerol as well as at low temperatures only amorphous precipitation was observed. Crystals in the form of hexagonal bipyramids were obtained in hanging-drop vapor-diffusion experiments conducted at 299 K where equal volumes of protein solution at 15–20 mg ml^{-1} [in 300 m*M* $(NH_4)_2SO_4$, 1 m*M* DTT, 20 m*M* BES pH 7.0] were mixed with a reservoir solution containing 46–52% saturated $(NH_4)_2SO_4$, 28–32%(*v*/*v*) glycerol, 20–100 m*M* BES pH 7.0. SecA crystals were harvested from the mother liquor after between two weeks and eight months of growth and frozen directly in liquid propane for low-temperature data collection without additional cryoprotection.

The crystals generally nucleated during the first 1–10 d of equilibration, but grew slowly over the course of 3–6 months to a limiting size of up to 400 × 400 × 150 µm (Fig. 2). Older crystals sometimes showed better local order in their lattice than fresh crystals, as evidenced by a substantial improvement in the scaling *B* factor for their diffraction data relative to that from a reference crystal. While useful crystals could be obtained from preparations showing more than 85% N-terminal homogeneity, the largest and most strongly diffracting crystals were obtained from preparations showing approximately 95% N-terminal homogeneity. Equivalent diffraction properties were observed with crystals mounted directly from the mother liquor or from a stabilization solution containing 54% saturated $(NH_4)_2SO_4$, 30%(*v*/*v*) glycerol, 20 m*M* BES pH 7.0 (±20 m*M* DTT).

Diffraction data were collected using a MAR 345 imaging-plate area detector on beamline ID2B at the European Synchrotron Radiation Facility (ESRF). Additional data sets were collected on beamlines X12B and X4A at the National Synchrotron Light Source at Brookhaven National Laboratory and on beamlines A1 and F1 at the Cornell High Energy Synchrotron Source (CHESS). The diffraction data were reduced using the program *DENZO* and scaled using the program *SCALEPACK* (Otwinowski & Minor, 1997).

The SecA crystals typically diffracted X-rays to a limiting resolution of 4 Å using a rotating-anode source and better than 3 Å using a synchrotron-radiation source (Table 1). While the diffraction properties of the crystals were stable during several days of X-ray exposure from a rotating-anode source at room temperature, severe decay was observed during the first 2 min of exposure on the synchrotron beamlines at the Cornell High Energy Synchrotron Source (CHESS) unless the crystals were frozen.

The SecA crystals possess the symmetry of the trigonal space group $P3_112$, with unit-cell parameters a = 130.8, b = 130.8, c = 150.4 Å at 100 K (after freezing in liquid propane). Given the presence of one SecA monomer per asymmetric unit, the observed unit-cell parameters correspond to a Matthews coefficient of 3.9 Å^3 Da^{-1} (Matthews, 1968) or a solvent content of 68%, assuming a specific volume of 0.74 cm^3 g^{-1} for the protein.

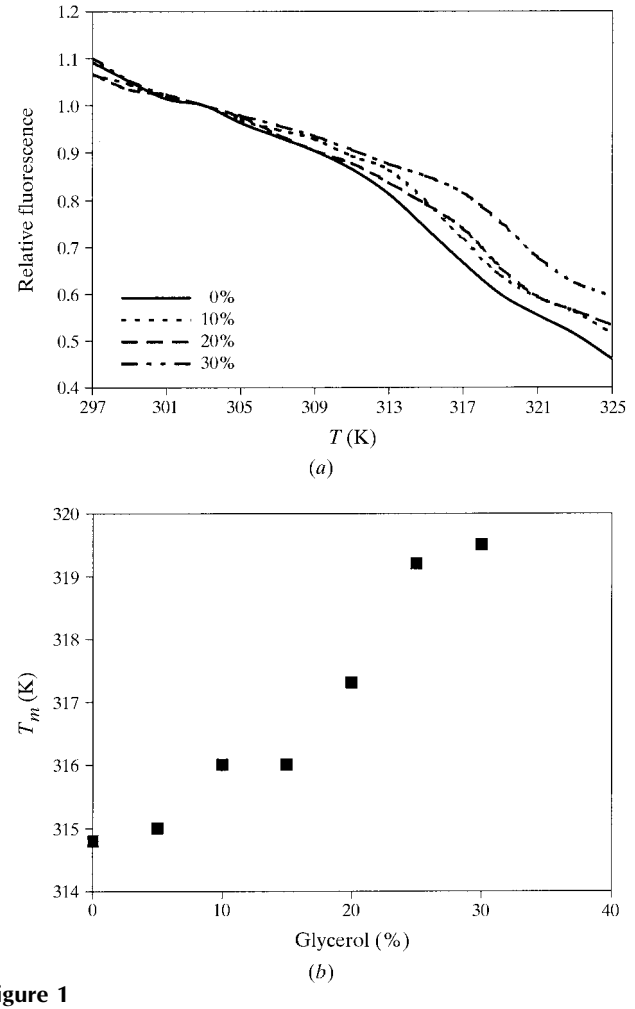

Figure 1
The endothermic conformational transition of *B. subtilis* SecA monitored as a function of glycerol concentration using fluorescence spectroscopy. (*a*) Thermal titration curves of SecA at varying glycerol concentration. The emission intensity at 340 nm was extracted from fluorescence spectra collected using an excitation wavelength of 280 nm. For details, refer to §4. (*b*) The inferred T_m of the endothermic transition is plotted against glycerol concentration.

6. Conclusions

The SecA protein, which is the ATP-driven motor of the bacterial translocation apparatus, proved to be extremely difficult to crystallize in a three-dimensional lattice that was sufficiently ordered to yield high-resolution diffraction data (Weaver *et al.*, 1992). Previous biochemical work has indicated that SecA possesses a high conformational flexibility necessary for performing its cellular functions (Ulbrandt *et al.*, 1992; Song & Kim, 1997). This flexibility may give rise to a dynamic structural heterogeneity which could represent a barrier to growth of high-quality crystals.

Based on CD and fluorescence measurements, it was proposed that *E. coli* SecA has a loose, unstable and possibly even partially unfolded tertiary structure in solution at temperatures above that of its endothermic conformational transition at about 315 K (Song & Kim, 1997); these conformational features are common to many proteins that insert into membranes. While a more compact and tightly ordered conformation of SecA is predominant below the temperature of the endothermic transition, a small percentage of the population will still adopt the more loosely organized high-temperature conformational state given the well behaved nature of the conformational equilibrium. The van't Hoff relationship dictates that the extent to which the enzyme occupies the more extended conformation will depend on the temperature offset relative to the T_m of the transition (*i.e.* $K \simeq \exp\{(\Delta H/R)[(1/T_m) - (1/T)]\}$, where K is the equilibrium constant, T is the temperature and ΔH is the enthalpy). Our fluorescence data show substantial elevation of the T_m of the endothermic transition of *B. subtilis* SecA in the presence of high concentrations of glycerol, indicating strong stabilization of the compact protease-resistant low-temperature conformation of the enzyme. As a result, conformational excursions of the enzyme into the more open conformation are at least partially reduced at any given temperature below the T_m in the presence of glycerol. As crystallization experiments at either 293 or 303 K resulted in only amorphous precipitate, the role of temperature in controlling the crystallization process is more complex than simply its effect on the equilibrium constant for the endothermic transition, as to be expected given the complex temperature dependence of the thermodynamic properties of water. In this context, it is obviously possible that the effect of a high glycerol content on the crystallization process may be more complex than simply stabilization against the endothermic transition of SecA. High glycerol content is also likely to suppress the dynamic fluctuation of individual surface loops on SecA (*i.e.* motions independent of the major endothermic conformational change). High glycerol content could also participate directly in the crystallization process by binding to the protein surface – which would be difficult to detect at 2.7 Å resolution – or indirectly by modulating the thermodynamic properties of the aqueous solution.

The results from fluorescence experiments on *B. subtilis* SecA are consistent with the 'structure-ordering' or 'structure-stabilizing' role that has been proposed for cosmotropic polyols and especially for glycerol (Gekko & Timasheff, 1981*a*,*b*; Santoro *et al.*, 1992). This effect has been attributed to preferential hydration of protein side chains compared with the backbone in the presence of the cosmotrope (Gekko & Timasheff, 1981*a*,*b*; Liu & Bolen, 1995; Wang & Bolen, 1997). Under these conditions, hydration forces can be expected to drive condensation of weakly ordered polypeptide loops onto the surface of the protein as well as closure of exposed clefts at domain–domain interfaces in order to minimize backbone interaction with solvent. Therefore, glycerol should stabilize maximally compact enzyme conformers that represent optimal species for crystallization. Several authors have advocated the use of glycerol as an additive to facilitate the crystallization of large proteins containing flexible domains, surface-exposed loops and disordered terminii (Sousa & Lafer, 1990; Sousa *et al.*, 1991; Sousa, 1995; Pechik *et al.*, 1993; Jeruzalmi & Steitz, 1997). In addition, a closely related property of cosmotropic polyols such as glycerol is the ability to suppress protein denaturation and subsequent aggregation, which could also contribute to promoting the growth of high-quality crystals.

Because of the inherent thermodynamic vagaries of protein crystallization reactions, it is difficult to establish a general cause-and-effect relationship based on the glycerol-dependent behavior of a single crystallization reaction. Given this difficulty, correlative data from a variety of systems is essential to evaluate whether glycerol is generally useful in promoting crystallization of conformationally dynamic proteins. In this paper, we show that high concentrations of glycerol stabilize the compact conformational ground state of the SecA ATPase from *B. subtilis*; we also observe that these same concentrations of glycerol are required to obtain high-quality crystals of the enzyme suitable for three-dimensional structure determination.

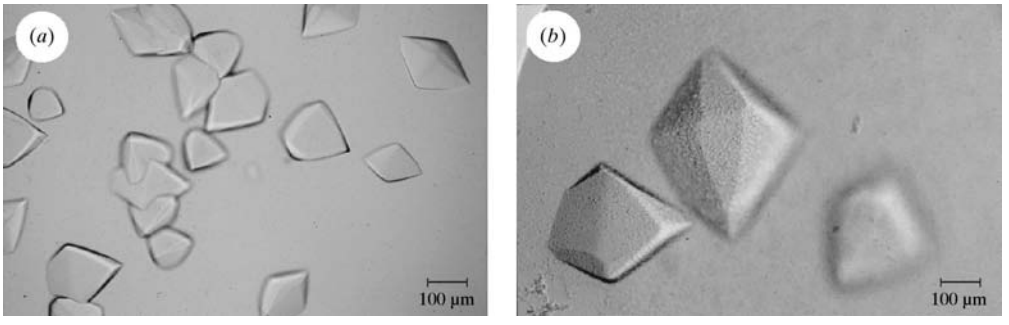

Figure 2
Hexagonal bipyramidal crystals of the SecA translocation ATPase from *B. subtilis* grown in ammonium sulfate and 30%(*v*/*v*) glycerol at neutral pH. (*a*) The crystals grew to dimensions of about 150 × 150 × 50 µm after two weeks of growth. (*b*) The crystals attained a limiting size of about 400 × 400 × 200 µm after 3–7 months of growth. During this lengthy growth period, an improvement in the diffraction power of the crystals was also often observed.

For support during data collection, we acknowledge Bjarne Rasmussen (ESRF), Malcolm Capel and Craig Ogata (NSLS), Bill Miller, Marian Szbenyi and Dan Theil (CHESS). We thank Troy Wingert for technical assistance with protein purification and crystallization, Drs Lothar Esser, Mischa Machius and Di Xia for advice and assistance, Carolyn Moomaw for N-terminal sequence analyses and the Deutsche Forschungsgemeinschaft for providing financial support for Dr Johannes Scheuring. Most of this work was performed while SW and JFH were research associates with JD in the Howard Hughes Medical Institute.

References

Beckmann, R., Bubeck, D., Grassucci, R., Penczek, P., Verschoor, A., Blobel, G. & Frank, J. (1997). *Science*, **278**, 2123–2126.
Blaauwen, T. den & Driessen, A. J. M. (1996). *Arch. Microbiol.* **165**, 1–8.
Blaauwen, T. den, Fekkes, P., de Wit, J. G., Kuiper, W. & Driessen, A. J. M. (1996). *Biochemistry*, **35**, 11994–12004.
Breukink, E., Nouwen, N., van Raalte, A., Mizushima, S., Tommassen, J. & de Kruijff, B. (1995). *J. Biol. Chem.* **270**, 7902–7907.
Cabelli, R. J., Chen, L., Tai, P. C. & Oliver, D. B. (1988). *Cell*, **55**, 683–692.
Cabelli, R. J., Dolan, K. M., Qian, L. P. & Oliver, D. B. (1991). *J. Biol. Chem.* **266**, 24420–24427.
Drenth, J. (1994). *Principles of Protein X-ray Crystallography*. New York: Springer–Verlag.
Driessen, A. J. M. (1992). *EMBO J.* **11**, 847–853.
Driessen, A. J. M. (1993). *Biochemistry*, **32**, 13190–13197.
Duong, F. & Wickner, W. (1997*a*). *EMBO J.* **16**, 2756–2768.
Duong, F. & Wickner, W. (1997*b*). *EMBO J.* **16**, 4871–4879.
Economou, A. & Wickner, W. (1994). *Cell*, **78**, 835–843.
Fekkes, P., van der Does, C. & Driessen, A. J. (1997). *EMBO J.* **16**, 6105–6113.
Gekko, K. & Timasheff, S. N. (1981*a*). *Biochemistry*, **20**, 4667–4676.
Gekko, K. & Timasheff, S. N. (1981*b*). *Biochemistry*, **20**, 4677–4686.
Hanein, D., Matlack, K. E., Jungnickel, B., Plath, K., Kalies, K. U., Miller, K. R., Rapoport, T. A. & Akey, C. W. (1996). *Cell*, **87**, 721–732.
Hartl, F. U., Lecker, S., Schiebel, E., Hendrick, J. P. & Wickner, W. (1990). *Cell*, **63**, 269–279.
Jeruzalmi, D. & Steitz, T. A. (1997). *J. Mol. Biol.* **274**, 748–756.
Joly, J., Leonard, M. R. & Wickner, W. (1994). *Proc. Natl Acad. Sci. USA*, **91**, 4703–4707.
Joly, J. C. & Wickner, W. (1993). *EMBO J.* **12**, 255–263.
Kimura, E., Akita, M., Matsuyama, S. & Mizushima, S. (1991). *J. Biol. Chem.* **266**, 6600–6606.
Lill, R., Dowhan, W. & Wickner, W. (1990). *Cell*, **60**, 271–280.
Liu, Y. & Bolen, D. W. (1995). *Biochemistry*, **34**, 12884–12891.
McNicholas, P., Rajapandi, T. & Oliver, D. (1995). *J. Bacteriol.* **177**, 7231–7237.
Manting, E. H., van der Does, C., Remigy, H., Engel, A. & Driessen A. J. M. (2000). *EMBO J.* **19**, 852–861.
Matthews, B. V. (1968). *J. Mol. Biol.* **33**, 491–497.
Meyer, T. H., Menetret, J. F., Breitling, R., Miller, K. R., Akey, C. W. & Rapoport, T. A. (1999) *J. Mol. Biol.* **285**, 1789–1800.
Mitchell, C. & Oliver, D. (1993). *Mol. Microbiol.* **10**, 483–497.
Oliver, D. B. (1993). *Mol. Microbiol.* **7**, 159–165.
Otwinowski, Z. & Minor, W. (1997). *Methods Enzymol.* **276**, 307–326.
Pechik, I., Nachman, J., Ingham, K. & Gilliland, G. L. (1993). *Proteins Struct. Funct. Genet.* **16**, 43–47.
Price, A., Economou, A., Duong, F. & Wickner, W. (1996). *J. Biol. Chem.* **271**, 31580–31584.
Ramamurthy, V., Dapic, V. & Oliver, D. (1998). *J. Bacteriol.* **180**, 6419–6423.
Sadaie, Y., Takamatsu, H., Nakamura, K. & Yamane, K. (1991). *Gene*, **98**, 101–105.
Santoro, M. M., Liu, Y., Khan, M. A. S., Hou, L.-X. & Bolen, D. W. (1992). *Biochemistry*, **31**, 5278–5283.
Shilton, B., Svergun, D. I., Volkov, V. V., Koch, M. H. J., Cusack, S. & Economou, A. (1998). *FEBS Lett.* **436**, 277–282.
Snyders, S., Ramamurthy, V. & Oliver, D. (1997). *J. Biol. Chem.* **272**, 11302–11306.
Song, M. & Kim, H. (1997). *J. Biochem.* **122**, 1010–1018.
Sousa, R. (1995). *Acta Cryst.* D**51**, 271–277.
Sousa, R. & Lafer, E. M. (1990). *Methods*, **1**, 50–56.
Sousa, R., Lafer, E. M. & Wang, B. C. (1991). *J. Cryst. Growth*, **110**, 237–246.
Takamatsu, H., Fuma, S., Nakamura, K., Sadaie, Y., Shinkai, A., Matsuyama, S., Mizushima, S. & Yamane, K. (1992). *J. Bacteriol.* **174**, 4308–4316.
Ulbrandt, N. D., London, E. & Oliver, D. B. (1992). *J. Biol. Chem.* **267**, 15184–15192.
Wang, A. & Bolen, D. W. (1997). *Biochemistry*, **36**, 9101–9108.
Weaver, A. J., McDowall, A. W., Oliver, D. B. & Deisenhofer, J. (1992). *J. Struct. Biol.* **109**, 87–96.
Wolk, J. P. van der, de Wit, J. G. & Driessen, A. J. M. (1997). *EMBO J.* **16**, 7297–7304.
Yoshida, M. & Amano, T. (1995). *FEBS Lett.* **359**, 1–5.